Strength and Stiffness of Cross-Laminated Timber (CLT) shear walls: State-of-the-art of analytical approaches

Ildiko Lukacs, Anders Björnfot, Roberto Tomasi

Department of Civil and Environmental Engineering, Faculty of Science and Technology (REALTEK), Norwegian University of Life Sciences, Ås, Norway

ABSTRACT

In the last years, the timber construction practice has been revived. Cross-laminated timber (CLT) plays a key role in this timber renaissance. CLT constructions has seen a noticeable increase in the last decade, especially in Europe, as it enables tall wooden buildings using a sustainable material. Unfortunately, a consequence of the rapid advancements of timber technologies and construction techniques of the past years is that modern timber engineering codes are struggling to keep up to date. Furthermore, the results of scientific research in this field is often inhomogeneous and fragmented, and do not help in proving that these new methods and construction techniques are reliable and safe to use.

To overcome this gap, COST Action FP1402 was created which main purpose is to create new, and improve on existing, knowledge of timber design and construction. This paper provides a summary of multiple fundamental aspects of design of CLT shear walls through a review of relevant scientific papers. This paper thus aims to be a "state-of-the-art" of available methods used to assess the load-carrying capacity and the displacement of CLT shear walls.

Keywords

Cross-laminated timber (CLT); CLT shear walls; analytical approaches; strength assessment methods; stiffness assessment methods; state-of-the-art.

1. INTRODUCTION

Cross-laminated timber (CLT) is an efficient wood product that is well suited for multi-story timber buildings due to its relative high strength and stiffness. Knowledge of CLT technologies and construction techniques has advanced quickly in the last few years but an absence of up-to-date CLT standards makes it difficult for engineers to design cost-efficient CLT constructions as design information is often limited to European Technical Approvals (ETA). To harmonize recent efforts in research and to consolidate a correct building practice, the COST Action FP1402 was established. FP1402 aims at deriving universal product parameters and design methods to verify the compliance of timber systems with requirements in terms of resistance, stability and serviceability asked for by designers, industry practitioners and authorities.

While equations for design of light timber frame shear walls and diaphragms are available in most codes or commentaries, no or little guidance on the in-plane stiffness of CLT diaphragms is given, e.g., the Eurocodes [1, 2] provide little information on the design of the lateral load-carrying system of CLT buildings [3]. Consequently, there is a need to explore design methods for CLT shear walls and floor diaphragms, which constitute the main structural elements in tall timber buildings [4, 5]. Floor diaphragms are typically considered as either fully flexible or rigid, depending on the relation between the maximum in-plane deformation of the floor diaphragm ($\Delta_{d,max}$) and the average inter-story drift ($\Delta_{L,ave}$) (Fig. 1). CLT diaphragms are often considered as rigid in relation to the stiffness of shear walls, see e.g. [6, 7, 8,], even though there is little information on its in-plane behavior [9].

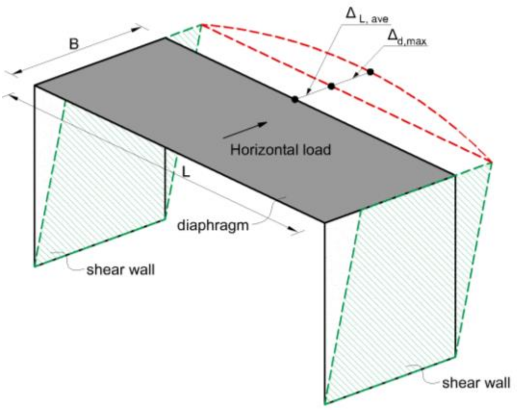

Diaphragm type	EUROPE EN 1998:2010 [2]	USA ASCE 7-10 [10] IBC 2012 [11] SDPWS 2008 [12]
Flexible	$\Delta_{d,max} \geq 1.1\Delta_{L,ave}$	$\Delta_{d,max} \geq 2\Delta_{L,ave}$
Rigid	$\Delta_{d,max} < 1.1\Delta_{L,ave}$	$\Delta_{d,max} \geq 0.5\Delta_{L,ave}$
Semi-rigid	–	$0.5 < \frac{\Delta_{d,max}}{\Delta_{L,ave}} < 2$

Figure 1. Diaphragm definition based on displacement of diaphragm versus inter-story drift, based on Moroder [3].

A general approach is to design for the case of either a rigid or a flexible diaphragm that gives the largest forces in shear walls. If the force in any shear wall differs by more than 15 % due to the change in the flexible and rigid diaphragm assumptions, then an envelope force approach should be used [13] where the design forces are based on the highest forces obtained from either the rigid or flexible case. However, neither assumption provides an accurate estimate of the lateral load distribution in case of semi-rigid diaphragms [9] which might lead to an underestimation of design forces since diaphragms are generally semi-rigid. [14]. By assigning the CLT diaphragm as either rigid or semi-rigid, lateral loads are distributed throughout diaphragms and shear walls in relation to the stiffness properties of each shear wall [14].

In the literature, there is currently a lack of a cohesive view on how to properly design CLT shear walls. As part of the research of COST Action FP1402, this paper summarizes multiple fundamental aspects of design of CLT shear walls through a review of several relevant scientific papers. This paper thus aims to be a "state-of-the-art" of methods used to assess the load-carrying capacity and the displacement of CLT shear walls.

2. STRENGTH OF CLT SHEAR WALLS

Design of CLT shear walls is performed by assessing its load-carrying capacity and its stiffness. Analytical methods for design of CLT shear walls are based on the different contributions of the shear wall deformation. Four contributions are typically considered (Fig. 2); translational (or slip), rotational (or rocking), panel shear and panel bending. For most shear wall configurations, the contribution of the in-plane panel shear and bending deformation are much smaller than the deformations from translation and rocking, which is governed by steel connections that typically exhibit a much softer behavior [15, 16, 17]. Verification of load-carrying capacity and stiffness of CLT shear walls mainly consists of equilibrium equations based on wall geometry, external loading and connection properties.

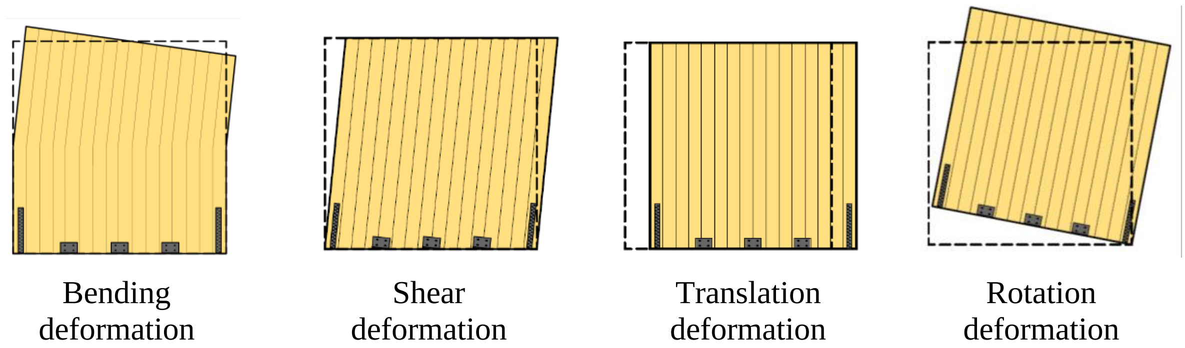

.

Figure 2. Illustration of the different contributions of the shear wall deformation.

2.1. Definitions & notations

To support the description of the different methods for strength and stiffness assessment, and to assist in comparing their inputs and results, a standardized shear wall is defined with generalized notations (Fig. 3). The shear wall is a CLT panel with width (w), height (h) and thickness (t) that is loaded by a lateral force (F) and a vertical load (q). The compressive strength (f_c) of the CLT panel and its elastic (E) and shear (G) modulus, along with the angle brackets (AB) and hold-downs (HD) are defined in Fig. 14. The angle brackets and hold-downs are described by their vertical strength (T), horizontal strength (H) and their stiffness in the vertical (k^V) and horizontal (k^H) directions.

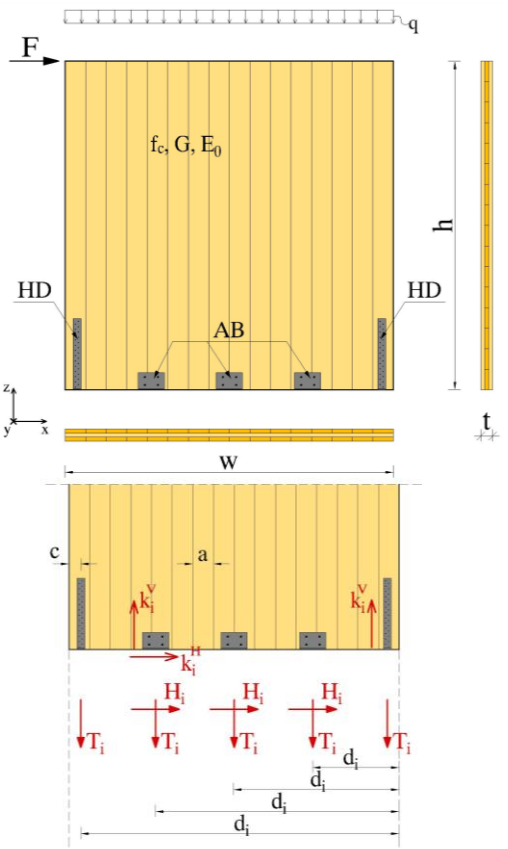

AB – angle bracket, steel connector
HD – hold-down, steel connector
n_{AB} – number of angle brackets
h – panel height [m]
w – panel width [m]
t – panel thickness [m]
F – horizontal force [N], i.e., shear wall capacity
q – uniformly distributed load [N/m]
c – edge distance [m]
d_i – distance from edge of panel to ith connector [m]
a – width of the timber board [m]
T_i – tensile strength of the ith connector [N]
H_i – horizontal strength of the ith connector [N]
k_i^V – vertical stiffness of the ith connector [N/m]
k_i^H – horizontal stiffness of the ith connector [N/m]
f_c – compressive strength of timber [MPa]
G – Shear modulus perpendicular to the grain [MPa]
E_0 – Elastic modulus parallel to the grain [MPa]

Figure 3. Definition of a standardized shear wall with notations used throughout this paper.

2.2. Methods for strength assessment

In the literature, several methods for calculating the load-carrying capacity of a CLT shear wall are identified. Common for these methods is that they are mainly based on static equilibrium equations and that the majority of methods consider the wall panel as rigid, i.e., the deformation of the CLT panel itself is disregarded in favor of the connections. If not explicitly stated, all of the methods resist overturning by hold-downs (HD), and translation by angle brackets (AB) exclusively as was first proposed by Ceccotti et al. [6]. This means that an interaction of vertical and horizontal forces in the connections are not typically considered as there is limited experimental data and no current design guidance (Reynolds et al. [18]). Thus the load-carrying capacity (F) of the CLT shear wall can be simplified as $F = min(F_R; F_T)$ where F_R and F_T denotes the load-carrying capacity by rotation and translation respectively. If not otherwise stated $F_T = H_i \cdot n$, where n is the number of angle brackets not used to resist shear wall rotation.

***Method A** – Casagrande et al.* *[19]*

Casagrande et al. [19] presented a simplified analytical method to evaluate the load-carrying capacity of a CLT shear wall based on rigid body rotation and static equilibrium between internal forces and the overturning moment ($F_R \cdot h$) (Fig. 4). With the point of rotation assumed at the panel edge, the force in the hold-down (T) due to a lateral (F_R) and vertical load (q) is calculated as:

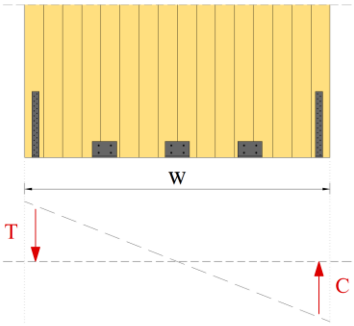

$$T = \frac{F_R \cdot h}{\tau \cdot w} - \frac{q \cdot w}{2} \tag{1}$$

Figure 4. The simplified analytical method as proposed in [19].

A lever arm coefficient, τ of 0.90 times the length of the wall was used by Casagrande et al. [19] to represent a reduction in width that takes into account the distance from the panel edge to the hold-down, giving the expression for the maximum lateral force (F_R) based on the vertical capacity of the hold-down (T):

$$F_R \cdot h = \left(T + \left(\frac{q \cdot w}{2}\right)\right) \cdot (0.9 \cdot w) \tag{2}$$

***Method B** – Tomasi* *[20]*

Tomasi [20] proposed a “Stress block” method, where the nonlinear stress distribution for wood in the compression zone is substituted by a rectangular stress block (Fig. 5). The unknown position of the neutral axis is denoted by x and Tomasi [20] defined the size of the “stress block” as $0.8 \cdot x$ from which a resultant compression force (C) is calculated (Eq. 3) based on the compression resistance parallel to the grain (f_c) and the width of the vertical lamellas (t_{ef}) of the CLT element. Using the tensile capacity (T) of the hold-down, the neutral axis (x) is then determined by transitional equilibrium (Eq. 4) resulting in the expression for x (Eq. 5).

Tomasi [20] thus assumes that the foundation is infinitely stiff compared to the CLT element. Ringhofer [21] and Schickhofer & Ringhofer [22] presented a similar “stress block” methods adding the possibility to consider a deformable CLT flooring underneath of the shear wall.

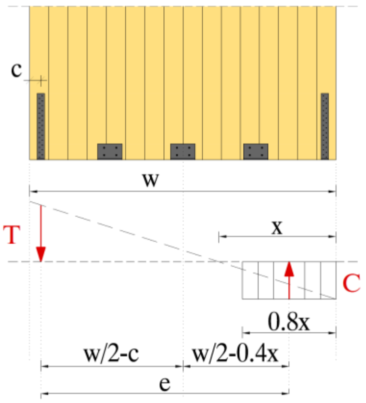

$$C = (0.8 \cdot x) \cdot f_c \cdot t_{ef} \tag{3}$$

$$C - q \cdot w - T = 0 \tag{4}$$

$$x = \frac{q \cdot w + T}{0.8 \cdot f_c \cdot t_{ef}} \tag{5}$$

Figure 5. Illustration of the “stress block” method as proposed in [20].

The tension force in the hold-down (T) is then determined by means of rotational equilibrium (Eq. 5) in the center of the panel:

$$-F_R \cdot h + T \cdot \left(\frac{w}{2} - c\right) + C \cdot \left(\frac{w}{2} - 0.4 \cdot x\right) = 0 \tag{6}$$

Using the expression in Eq. 3 for the resultant compressive force (C) and the expression in Eq. 5 for the neutral position (x), the total lateral force on the wall is then calculated as:

$$F_R \cdot h = T \cdot \left(\frac{w}{2} - c\right) + (q \cdot w + T) \cdot \left(\frac{w}{2} - \frac{(q \cdot w + T)}{2 \cdot f_c \cdot t_{ef}}\right) \tag{7}$$

***Method C** – Wallner-Novak et al. [15]*

Wallner-Novak et al. [15] proposed a similar method but with a different length of the compression zone (x) corresponding to ¼ of the wall width (Fig. 6), and a 10 % reduced effect of the vertical load (q) emanating from the partial safety factor for permanent loads. Rotational equilibrium (Eq. 8) yields the expression (Eq. 10) for the total lateral force (F_R):

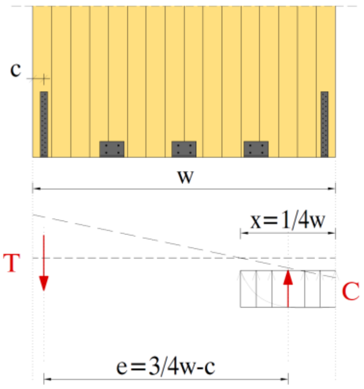

$$T = \frac{F_R \cdot h}{e} - \frac{(0.9 \cdot q) \cdot w}{2} \tag{8}$$

$$e = \frac{3}{4} \cdot w - c \tag{9}$$

$$F_R \cdot h = \left(T + \frac{(0.9 \cdot q) \cdot w}{2}\right) \cdot \left(\frac{3}{4} \cdot w - c\right) \tag{10}$$

Figure 6. Illustration of the internal lever arm (e) as proposed in [15].

In contrary to the general sliding resistance (F_T) calculated as the sum of the resistance of the angle brackets, Wallner-Novak et al. [15] included the contribution of friction (with a friction coefficient μ = 0.4) of the vertical load (q) to the sliding resistance of the shear wall (Eq. 11):

$$F_T = \sum H_i + \mu \cdot (0.9 \cdot q) \cdot w \tag{11}$$

<u>Method D</u> *<u>– Pei et al. [23]</u>*

Pei et al. [23] presented a method that considers the CLT panel as a rigid body rotating around one of its corners (Fig. 7). Pei et al. [24], Shen et al. [25], Karakabeyli & Douglas [26] and Gavric & Popovski [27] all presented similar methods. It should be specifically noted that the proposed simplified kinematic method does not explicitly consider the sliding resistance of the shear wall. Instead a connection resistance was "back-calibrated" by comparing the model hysteretic obtained from numerical modelling with experimental measurements [23, 24] so that the load-carrying capacity is limited by rigid body rotation around one of the panels corners. Therefore, care should be taken when comparing this method to other similar methods.

To determine the lateral force, the connector's elongation and stiffness/strength is considered. The tensile strength of each connector is proportional with the distance of the connector from the panel edge. A triangular distribution of the connector displacement is considered based on that the furthest connector (the left hold-down according to Fig. 7) reaches its total elastic tensile strength (T). Imagining the remaining connections as elastic springs, they will elongate based on a triangular distribution and thus their tensile strength is proportional with their distance (d_i) from the rotational point. The calculation steps for Method D are as follows:

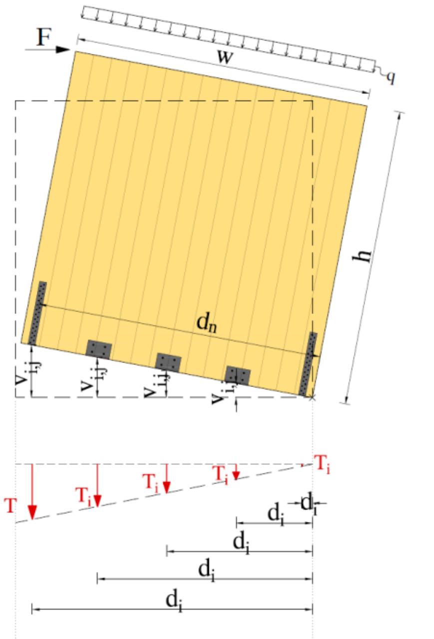

1. Determine the tensile strength (T) of the connector furthest from the point of rotation.
2. Calculate the elongation ($v_{i,y}$) for the hold-down based on its vertical stiffness (k^{v}) and capacity (T).
3. Calculate the elongation ($v_{i,y}$) for each connector based on a triangular distribution.
4. Calculate the tensile strength for each connector based on its stiffness ($T_i = v_{i,y} \cdot k_i^V$).
5. Calculate the total rotational resistance in terms of the total lateral load (F_R):

$$F_R \cdot h = \sum_{i=1}^{n} T_i \cdot d_i + \frac{q \cdot w}{2} \cdot d_n \tag{12}$$

where d_n is the distance from the panel edge to the furthest connector, which typically is the hold-down.

Figure 7. Illustration of, and calculation steps for Method D based on [23].

***Method E** – Reynolds et al. [18]*

Reynolds et al. [18] presented a method similar to Method D with a triangular distribution of the tensile capacity but with the addition of a compressive zone (Fig. 8). The calculation steps are; 1) determine the tensile strength (T) of the connector furthest from the point of rotation, 2) calculate the tensile capacity (T_i) of remaining connectors based on a triangular distribution (Eq. 13), 3) calculate the compression zone (x) of the wall (Eq. 14), and 4) determine the lateral resistance (F_R) of the shear wall (Eq. 15).

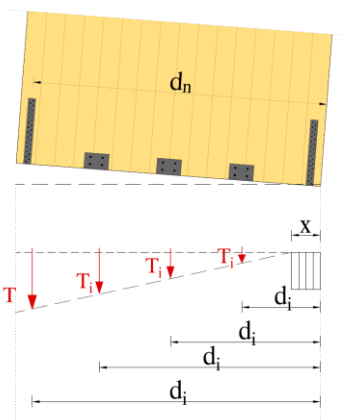

$$T_i = T \cdot \frac{d_i}{d_n} \tag{13}$$

where d_n is the distance from the panel edge to the furthest connector, and where T_i should not exceed the maximum capacity of the actual connector

$$x = \frac{q \cdot w + \sum T_i}{f_c \cdot t_{ef}} \tag{14}$$

$$F_R \cdot h = \sum_{i=1}^{n} T_i \cdot \left(d_i - \frac{x}{2}\right) + \frac{q \cdot w^2}{2} - (q \cdot w) \cdot \frac{x}{2} \tag{15}$$

Figure 8. Triangular distribution of tensile capacity as proposed by [18].

***Method F** – Reynolds et al. [18]*

Reynolds et al. [18] presented a method combining the kinematic equilibrium of Method D with a compressive zone of ⅓ of the panel width, similar to Methods B and C. This method only considers the resistance of the connectors placed in a "tensile zone" a distance of ⅓ of the width from the panel edge (Fig. 9). Assuming that the resultant force from the vertical load is centered in the panel, and defining the distance (d_i) to each connector in the "tensile zone", the lateral load-carrying capacity (F_R) can be calculated as:

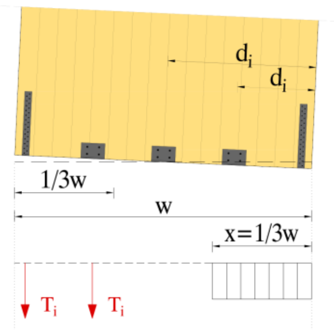

$$F_R \cdot h = \sum_{i=1}^{n} T_i \cdot \left(d_i - \frac{w}{6}\right) + \frac{q \cdot w^2}{3} \tag{16}$$

T_i – tensile strength of the connector furthest from the compression zone.

$d_i - \frac{2 \cdot w}{3} < d_i < w.$

Figure 9. Illustration of compression and "tensile" zones based on [18].

In this case, only the angle brackets outside of the tensile zone are available to resist sliding of the wall. However, contrary to the general sliding resistance (F_T) calculated as the sum of the resistance of the angle brackets, Reynolds et al. [18] included the contribution of friction (with a friction coefficient = 0.2) to the sliding resistance of the shear wall (Eq. 17):

$$F_T = \sum H_i + 0.2 \cdot \left(\sum T_i + q \cdot w\right) \tag{17}$$

***Method G** – Reynolds et al. [18]*

Reynolds et al. [18] presented another method similar to Method F but with a reduced compression zone (Eq. 18). In addition, the amount of connectors providing overturning resistance is increased to encompass all connectors outside of the compression zone (Fig. 10) with the exception that *"any connectors required to resist sliding are excluded"* [18]. The tensile resistance of each connector is taken as their maximum elastic capacity. Using a simple rotational equilibrium then gives the lateral resistance of the shear wall (Eq. 19). The sliding resistance of the wall is calculated in the same manner as for Method F (see Eq. 17).

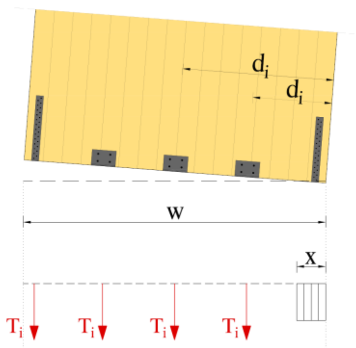

$$x = \frac{q \cdot w + \sum T_i}{f_c \cdot t_{ef}} \tag{18}$$

$\sum T_i$ – sum of vertical strength of the connectors activated in rotation

$$F_R \cdot h = \sum_{i=1}^{n} T_i \cdot \left(d_i - \frac{x}{2}\right) + \frac{q \cdot w^2}{2} - (q \cdot w) \cdot \frac{x}{2} \tag{19}$$

where $d_i > x$ as only connectors within the tension zone are considered.

Figure 10. Suggested method with extended "tensile" zone based on [18].

***Method H** – Gavric & Popovski [27]*

Gavric & Popovski [27] argued that the current proposed methods are too simplistic as they do not consider the interaction of shear and tension forces in the connectors. The proposed method considers interaction of shear and tension forces specifically in the angle brackets as tests showed that hold-downs does not provide any significant resistance in the shear direction [27]. An iterative process (Fig. 11) was applied to calculate a so called unreduced factored wall lateral resistance (F^*) and then iteratively reducing the "real" lateral load (F) until the interaction (circular or triangular) of shear and tension forces in angle brackets are within its limit. Rinaldin & Fragiacomo [28] analyzed the interaction domain and proposed a circular interaction to the power of two, as the most appropriate, but for ease of calculation, this paper will use the triangular verification of interaction (Eq. 20).

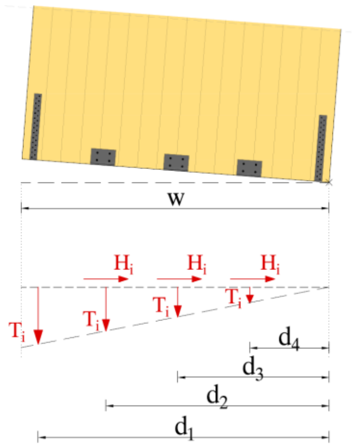

1. Calculate the resistance to sliding, F_T^* (Eq. 21)
2. Calculate the resistance to rotation F_R^* (Eq.22)
3. Specify $F^* = min\{F_T^*; F_R^*\}$
4. Assume reduced "real" resistance $F < F^*$
5. Calculate reduced H_i^* and T_{i+1}^*
6. Iterate until interaction of shear and tension in the most loaded angle bracket is verified.

$$\frac{H_i^*}{H_i} + \frac{T_i^*}{T_i} \leq 1 \tag{20}$$

Figure 11. Suggested iterative method as suggested by [27].

$$F_T^* = n_{AB} \cdot H_i \tag{21}$$

$$F_R^* = \left(\frac{q \cdot w^2}{2 \cdot h}\right) + \frac{T_1 \cdot d_1}{h} + \frac{T_{i+1}}{d_1 \cdot h} \cdot \sum (d_{i+1})^2 \tag{22}$$

***Method I** – Schickhofer et al. [29]*

Schickhofer et al. [29] presented a theoretical method (Fig 12) assuming a linear elastic and continuous behavior of the bottom joint [30]. Distributing the overturning moment from the lateral load (F_R) and including the contributing of the vertical load (q) makes it possible to evaluate the length of the tensile zone (l_T) (Eq. 24) and the tensile force (T) in the hold-down by equilibrium equations (Eq. 25). Using the maximum tensile capacity of the hold-down, the lateral resistance (F) can then be calculated.

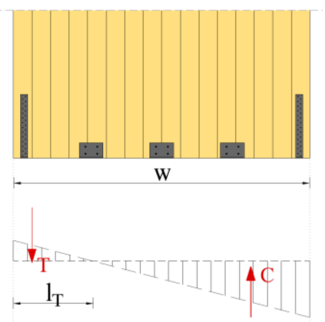

T – tensile load in hold down connector

$$T = \left(\frac{6 \cdot F_R \cdot h}{w^2} - q\right) \cdot \frac{l_T}{2} \tag{23}$$

where l_T is the length of the tension zone

$$l_T = \frac{1}{2} - \frac{q \cdot w^3}{12 \cdot F_T \cdot h} \tag{24}$$

$$T = \frac{3 \cdot F_R \cdot h - q \cdot w^2}{2 \cdot w} + \frac{q^2 \cdot w^3}{24 \cdot F_R \cdot h} \tag{25}$$

Figure 12. Suggested theoretical method based on [29].

***Method J** – Schickhofer et al. 2010 [29]*

Schickhofer et al. [29] presented a method combining a triangular compression zone with tensile bracing (Fig 13), depicting a situation where the lateral force is just large enough to cause the wall to rotate. The problem has three unknowns; the length of the compression zone (*x*), the maximum compressive force at the corner of the panel (N_c) and the load in the tensile bracing (*T*). However, with only two equilibrium equations being available, two solutions to the problem was proposed. The first solution (Eq. 26) assumes that the tensile bracing reaches its ultimate elastic capacity (*T*) in which case the lateral load ($F_{R,1}$) is limited by the maximum compressive stress at the corner of the panel ($N_c \leq f_c \cdot A_{ef}$) where A_{ef} is the effective area per length m shear wall, i.e., $A_{ef} = t_{ef} \cdot 1\ m$.

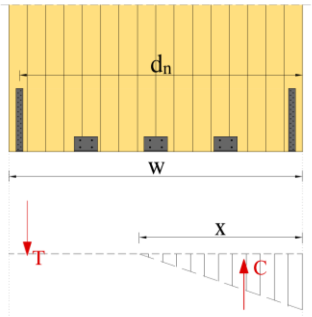

Solution I: Solve for $F_{R,I}$ by limiting N_c to $f_c{\cdot}A_{ef}$

$$N_c = \frac{4\cdot(q\cdot w)^2 + 8\cdot q\cdot w\cdot T + 4\cdot T^2}{3\cdot w\cdot(q\cdot w + T) - 6\cdot(F_{R,I}\cdot h - T\cdot d_n)} \tag{26}$$

Solution II*:* Solve for $F_{R,II}$ by limiting *T* to the capacity of the connector furthest from the compression edge:

$$T = \frac{1}{8}\cdot[-8\cdot(q\cdot w) + N_c\cdot(3\cdot w + 6\cdot e)] - \frac{\sqrt{3}}{8}\cdot\sqrt{N_c\cdot\left[N_c\cdot(3\cdot w^2 + 12\cdot w\cdot e + 12\cdot e^2) - \left(32\cdot\left((F_{R,II}\cdot h) + (q\cdot w\cdot e)\right)\right)\right]} \tag{27}$$

Figure 13. Suggested method based on [29].

The second solution (Eq. 27) assumes that the corner of the panel (Fig. 13) reaches its ultimate compressive capacity (f_c) in which case the lateral load ($F_{R,II}$) by limiting (*T*) to the tensile capacity of tensile bracing. In Eq. 27, the lever arm *e* is calculated as $e = d_n - w/2$. The lateral capacity of the shear wall with respect to rotation is then evaluated as $F_R = min(F_{R,I}; F_{R,II})$. Tamagone et al. [31] proposed a similar method utilizing the same failure modes but instead an iterative process was proposed to calculate the reaction force in the connections by varying the position of the natural axis. As this method requires the use of Finite Element software for its calibration, it is out of scope of this paper.

2.3. Comparison of strength methods

A calculation example is used to provide an indication of differences between the presented analytical methods. The comparison is based on a standard shear wall setup (Fig. 14) anchored to a concrete foundation with hold-downs (HD) and angle brackets (AB). The connectors used in this example are named HD620 and AB200, which is analogous with the connectors tested in Tomasi [32] and Tomasi & Smith [33]. For comparison, a 3-layered square (2500x2500 mm) CLT panel with a total thickness of 90 mm was used. The connections are placed on one side of the shear wall only. Maximum values based on tests were used for the connectors' tensile strength and stiffness while the characteristic value of the compressive strength parallel to the grain was used for the CLT panel.

Test results for the example shear wall is presented in [32, 34]. Test result for the vertical strength of the angle bracket is not available, but according to Gavric & Popovski [27] it can be assumed that the vertical capacity equals its horizontal capacity, which is also supported by test results [33]. Method D includes the vertical stiffness of the angle brackets for which no test data was found. In this case, a vertical stiffness value of a softer angle bracket was used which coincide with other tested connectors [32, 33].

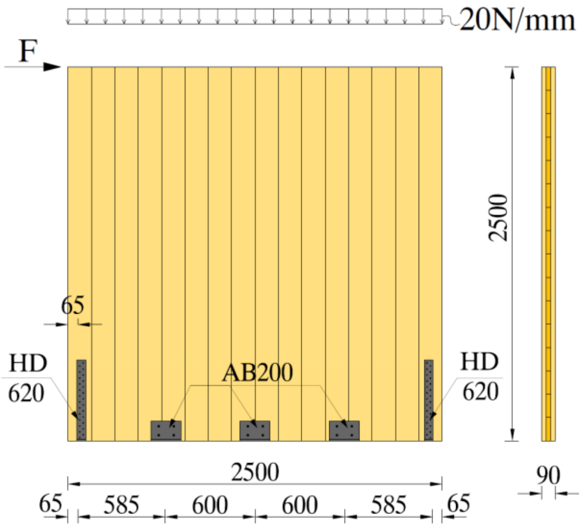

h = 2500 mm | w = 2500 mm | t = 90 mm
t_{ef} = 60 mm | a = 150 mm | $c = d_1$ = 65 mm
d_2 = 650 mm | d_3 = 1250 mm
d_4 = 1850 mm | d_5 = 2435 mm
q = 20 kN/m | n_{AB} = 3
$T_{i,HD}$ = 108.28 kN (vertical strength of HD)
$T_{i,AB}$ = 58.64 kN (vertical strength of AB)
$H_{i,AB}$ = 58.64 kN (horizontal strength of AB)
$k^V_{i,HD}$ = 9.07 kN/mm
$k^V_{i,AB}$ = 0.82 kN/mm | $k^H_{i,AB}$ = 6.07 kN/mm
G = 650 MPa | E = 11600 MPa
f_c = 21 MPa

Figure 14. Example shear wall with geometry and material data.

Based on data presented in Fig. 14, the lateral capacity in the tension and shear directions for the 10 different methods are illustrated in Fig. 15. The example wall has strong angle brackets in the shear direction which means that the load-carrying capacity of Methods A, B, C, I and J in translation is much higher than the load-carrying capacity for the respective wall in rotation.

Methods D represents a special case where an unmodified tensile strength based on tests was used to evaluate the wall capacity which is not what was suggested by [27]. However, at least for this wall setup, this approximation provides adequate results.

For Method H, the lateral load-capacity is evaluated based on a triangular interaction of the resistance in tension and shear. The Methods C, E, F and G all consider the increased shear capacity due to friction. Methods E, F, G represents a special case as the lateral load-carrying capacity is evaluated from the connectors providing overturning resistance that are not necessary to resist sliding [18]. For the considered wall setup, two angle brackets are required to resist sliding in Methods E and F, which means that the vertical capacity of one angle brackets is used to increase the capacity in rotation.

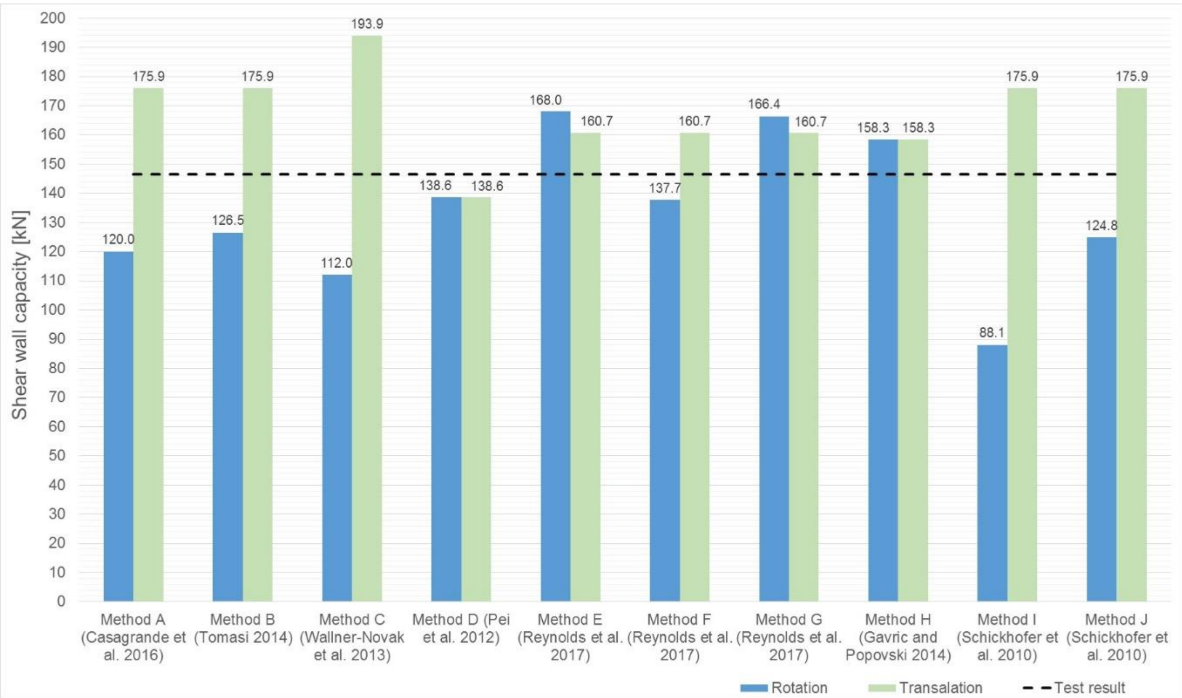

Figure 15. Rotational and shear capacities calculated from the 10 strength methods.

3. STIFFNESS OF CLT SHEAR WALLS

The force-displacement relation determines the stiffness of a shear wall. By knowing the maximum force acting on the shear wall, and the stiffness of the connectors, the wall displacement can be calculated. Analytical methods for the displacement of CLT shear walls are based on the different contributions to shear wall deformation (Fig. 2); translational Δ_T (or slip), rotational Δ_R (or rocking), panel shear Δ_S and panel bending Δ_B. Due to the relatively high in-plane stiffness of the CLT element, the rocking mechanism is generally dominant but different shear wall geometries, hold-downs and angle brackets with different strength and stiffness characteristics can have substantial effect [15, 16, 17].

3.1. Methods for stiffness assessment

In the literature, five methods for assessing the stiffness of CLT shear wall are identified; Casagrande et al. [19], Hummel et al. [35], Wallner-Novak et al. [15], Gavric et al. [36], Flatcher & Schickhofer [37]. If not otherwise stated, the state-of-the-art use the generalized notations previously presented in Fig. 3 and the total wall displacement is calculated as:

$$\Delta_{TOT} = \Delta_B + \Delta_s + \Delta_T + \Delta_R \tag{29}$$

Method I *– Casagrande et al. [19]*

Casagrande et al. [19] considered the contribution of the in-plane shear deformation (Δ_S), rigid-body translation (Δ_T) and rigid-body rotation (Δ_R) which is analogous to simplifications made by, e.g. Vessby [38] and Reynolds et al [39]. Similar to the assessment of the load-carrying capacity (presented as Method A above), Method I applies a level arm of 90 % of the width of the panel to calculate the rocking deformation. The different contributions to shear wall deformation are calculated as:

$$\Delta_T = \frac{F}{k_{AB}^{H} \cdot n_{AB}} \tag{30}$$

$$\Delta_S = \frac{F \cdot h}{G \cdot t \cdot w} \tag{31}$$

$$\Delta_R = \left(\frac{F \cdot h}{(0.9 \cdot w)} - \frac{q \cdot w}{2}\right) \cdot \frac{h}{k_{HD}^{V} \cdot (0.9 \cdot w)} \tag{32}$$

Method II *– Hummel et al. [35]*

Besides the shear deformation of the CLT panel, Method II also considers rotation/rocking of the wall panel due to tensile anchoring and contact, and slip of the wall panel due to shear anchoring. Method II also considers the bending deformation of the CLT panel (Fig. 2). The same contributions of deformations are also presented in Hummel [16], Seim et al. [40], and Hummel & Seim [41].

For the shear deformation, a reduced effective shear modulus of the CLT wall panel is considered. Hummel et al. [35] also considers the increased panel flexibility occurring from an elastic foundation where two cases are considered; 1) a rigid foundation (e.g., a concrete slab), and 2) an elastic foundation (e.g., a timber floor between stories with an elastic intermediate layer). The different contributions to shear wall deformation are calculated as:

$$\Delta_B = \frac{F \cdot h}{3 \cdot EI_{ef}} \tag{33}$$

$$\Delta_S = \frac{F \cdot h}{GA_{ef}} \tag{34}$$

$$\Delta_R = \begin{cases} \frac{h}{(w-2\cdot c)} \cdot \frac{max\left\{F \cdot \frac{h}{(w-2\cdot c)} - \frac{q \cdot w}{2};0\right\}}{k_{HD}^{v}} - rigid\ foundation \\ \frac{h^2}{d_i - l_c/3} \cdot \frac{2 \cdot F}{k_D \cdot l_c^2} - elastic\ foundation \end{cases} \tag{35}$$

$$\Delta_T = \frac{F}{n_{AB} \cdot k_{AB}^{h}} \tag{36}$$

The flexural stiffness is determined based on Eq. 37, where t_{ef} is the thickness of the vertical layers and w is the width of the CLT wall panel.

$$EI_{ef} = E_0 \cdot \left[\frac{t_{ef} \cdot w^3}{12}\right] \tag{37}$$

The shear stiffness is determined based on an effective shear modulus, G_{eff}, and the gross shear area, A, where a is the average width of the lamellae. Based on the thickness of the lamella the width a can vary between 80 and 240 mm, see for example [42]. The effective shear modulus was derived by Schickhofer et al. [29]:

$$GA_{ef} = G_{eff} \cdot A = \frac{G}{1+6\cdot\left[0.32\cdot\left(\frac{t}{a}\right)^{-0.77}\right]\cdot\left(\frac{t}{a}\right)^{2}} \cdot A, \text{ where } A = t \cdot w \tag{38}$$

A typical CLT shear wall with rigid/elastic is shown in Fig. 16. The rocking deformation can be calculated as presented in Eq. 35 for both foundation types.

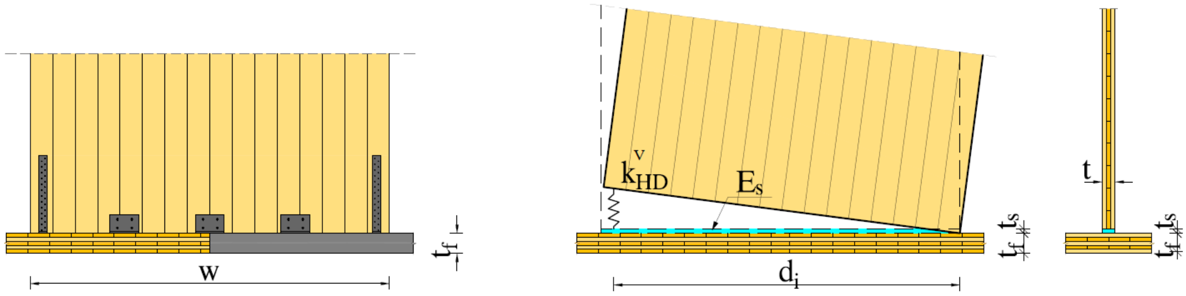

Figure 16. CLT wall with rigid foundation (left) and elastic intermediate layer (right). Illustrations based on Hummel et al. [35].

In the case of the elastic foundation, the width of the elastic intermediate layer (b_S), the E-modulus of the layer (E_S) and the length of pressure zone (l_c) is required. Two cases are distinguished for the width (b_S), one for the case of an exterior wall and one for an interior wall, (Eq. 39a,b) where t_f is the thickness of the floor element (Fig. 16). The E-modulus (E_S) can, for example, be for the elastic material Sylodyn, a common elastic intermediate layer used in CLT walls systems. The use of the elastic intermediate layer contributes to an increased rocking deformation due to the reduced stiffness (k_D) of the elastic foundation (Eq. 40).

$$b_s = t + \frac{1}{4} t_f \text{ – for exterior wall} \tag{39a}$$

$$b_s = t + \frac{1}{2} t_f \text{ – for interior wall} \tag{39b}$$

$$k_D = \frac{E_S \cdot b_S}{t_S} \tag{40}$$

***Method III** – Wallner-Novak et al. [15]*

Method III is presented by Wallner-Novak et al. [15] which considers the same contributions as Method II, with only a slight difference in the definition of the shear stiffness of the CLT panel due to a reduced shear modulus. The total displacement is calculated based on panel bending and shear as well as contributions from translation and rocking deformation:

$$\Delta_B = \frac{F \cdot h^3}{3 \cdot EI_{ef}} \tag{41}$$

$$\Delta_S = \frac{F \cdot h}{GA} \tag{42}$$

$$\Delta_T = \frac{F}{n_{AB} \cdot k_{AB}^H} \tag{43}$$

$$\Delta_R = \left[\frac{F \cdot h}{w} - \frac{q \cdot w}{2}\right] \cdot \frac{h}{w \cdot k_{HD}^V} \quad (44)$$

The bending stiffness (EI_{ef}) used in Eq. 41 is calculated according to Eq. 37 while the shear stiffness used in Eq. 42 is determined using a 25% reduction of the shear modulus:

$$GA = (0.75 \cdot G) \cdot (t \cdot w) \quad (45)$$

***Method IV** – Gavric et al. [36]*

This method was originally presented by Gavric et al. [43]. Gavric et al. [36], who argued that previous methods fail to take into account the tensile characteristics of angle brackets, proposed a method that takes into account all the stiffness and strength components of hold-downs and angle brackets also in their weaker directions. By introducing a vertical stiffness of angle brackets, a friction coefficient to reduce sliding, and a shape reduction factor of 1.2 for the shear deformations, the deformations can be calculated as:

$$\Delta_B = \frac{F \cdot h^3}{3 \cdot EI_{ef}} \quad (46)$$

$$\Delta_S = \frac{1.2 \cdot F \cdot h}{GA_{ef}} \quad (47)$$

$$\Delta_T = \frac{F - \mu \cdot q \cdot w}{n_{AB} \cdot k_{AB}^H} \quad (48)$$

$$\Delta_R = \frac{\left(F \cdot h - q \cdot \frac{w^2}{2}\right) \cdot h}{\sum k_{HD}^V \cdot d_i^2 + \sum k_{AB}^V \cdot d_i^2} \quad (49)$$

As in Method III, here also, the bending stiffness (EI_{ef}) in the bending deformation is calculated according to Eq. 37. According to Gavric et al. [36], the shear stiffness (GA_{ef}), is calculated with a shear modulus (G) equal to 0.69 GPa, and an effective shear area (A_{ef}), which is considering just the vertical layers, is calculated as:

$$A_{ef} = t_{ef} \cdot w \quad (50)$$

In translation, a friction coefficient (μ) of 0.3 is used. In rotation the panel is considered rigid, and rotating around a corner of the wall, similar to the strength Method D. However, in calculating the stiffness properties of the connectors, Gavric et al. [36, 43] also considers the non-linear behavior of the force-displacement curve, suggesting that the stiffness of each connector is evaluated based on the actual deformation of each connector. For this purpose, three different stiffness ranges were proposed (compare Fig. 17); with an initial elastic stiffness, a plastic stiffness until maximum load, and a negative stiffness phase until connection failure. The sum of these evaluated stiffnesses at certain deformation intervals where then used to calculated the rotation deformation (Eq. 49).

Method V *– Flatscher & Schickhofer [37]*

Flatscher & Schickhofer [37], and Flatscher [30] proposed a new displacement-based calculation method for predicting the total load-displacement behavior of a CLT shear wall. The fundamental difference of this method compared to force-based methods is that the sliding and rocking behavior cannot be analyzed separately. Similar to the methods described in Gavric et al. [36, 43] and Pei et al. [23], a rigid CLT body was assumed with a point of rotation at the lower corner of the wall element to predict the behavior of the connections' (Fig. 17).

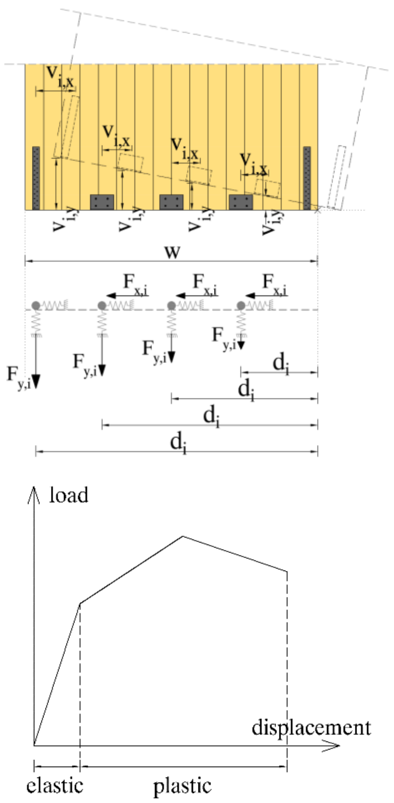

1. Assume a ratio p for the contribution of Δ_T and Δ_R to the total connection based deformation v_{con}.
2. Calculate the deformation of each connector in the shear ($v_{i,x}$) and tensile directions ($v_{i,y}$).

$$v_{i,x} = \Delta_T = p \cdot v_{con} \tag{51}$$

$$v_{i,y} = d_i \cdot \frac{(1-p) \cdot v_{con}}{h} \tag{52}$$

3. Evaluate a force $F_{x,i}$ and $F_{y,i}$ of each connector from their respective load-deformation relation.

$$F_{x,i} = f(v_i^x) = k_i^H \cdot v_{i,x} \tag{53}$$

$$F_{y,i} = f(v_i^y) = k_i^V \cdot v_{i,y} \tag{54}$$

4. Calculate the total lateral load on the wall based on sliding (F_T) and rocking (F_R).

$$F_T = \sum F_{x,i} + \left(\sum F_{y,i} + q \cdot w\right) \cdot \mu \tag{55}$$

$$F_R = \frac{1}{h} \cdot \left[\sum\left(F_{y,i} \cdot d_i\right) + \frac{q \cdot w^2}{2}\right] \tag{56}$$

5. As only one lateral force can be active at a time, iterate until $F_T = F_R$ by changing the ratio p.

Figure 17. Proposed displacement-based method showing the wall setup (based on [37, 30]) and a schematic force-displacement curve for a connector (inspired by [36]).

Evaluation of the maximum lateral force based on either sliding or rotation was made through an iterative process (Fig. 17). Flatscher [30] proposed that the strength and deformation characteristics of the connections is evaluated based on a multi-linear approximation of the load-deformation curve taking into account the plasticization of connectors (Fig. 17). Finally the contributions to deformation from panel shear and bending are calculated as

$$\Delta_S = \frac{F \cdot h}{G^* \cdot w \cdot t} \tag{57}$$

$$\Delta_B = \frac{4 \cdot F \cdot h^3}{E_0 \cdot w^3 \cdot t_{ef}} \tag{58}$$

The shear contribution is depending on an effective shear modulus, G^* (Eq. 59) based on [1], where p_s depends on the number of layers (0.53 for a 3 layered CLT element and 0.43 for a 5 layered CLT element).

$$G^* = \frac{G}{1 + 6 \cdot p_S \cdot \left(\frac{t}{a}\right)^{1.21}} \tag{59}$$

3.2. Comparison of stiffness methods

The stiffness methods are compared with each other using the load-deformation relation of the wall setup presented in Fig. 14 with an ultimate lateral resistance of 146.6 kN [32, 34]. The total displacement for each method is calculated as the sum of the displacement mechanisms (Fig. 2), bending, shear, translation and rotation according to Eq. 29. In Fig. 18, the results obtained for each method are illustrated as a load-deformation behavior and as a contribution by each deformation mechanism at ultimate load. The initial higher elastic stiffness of Fig. 18 can be explained by the positive contribution of the vertical load. When the lateral force is large enough to cause the wall to rotate, the positive impact of the vertical load is lost because the hold-down is activated and the stiffness of the wall is reduced. This contribution has been taken into consideration for each method so as to get a better correlation with the test results.

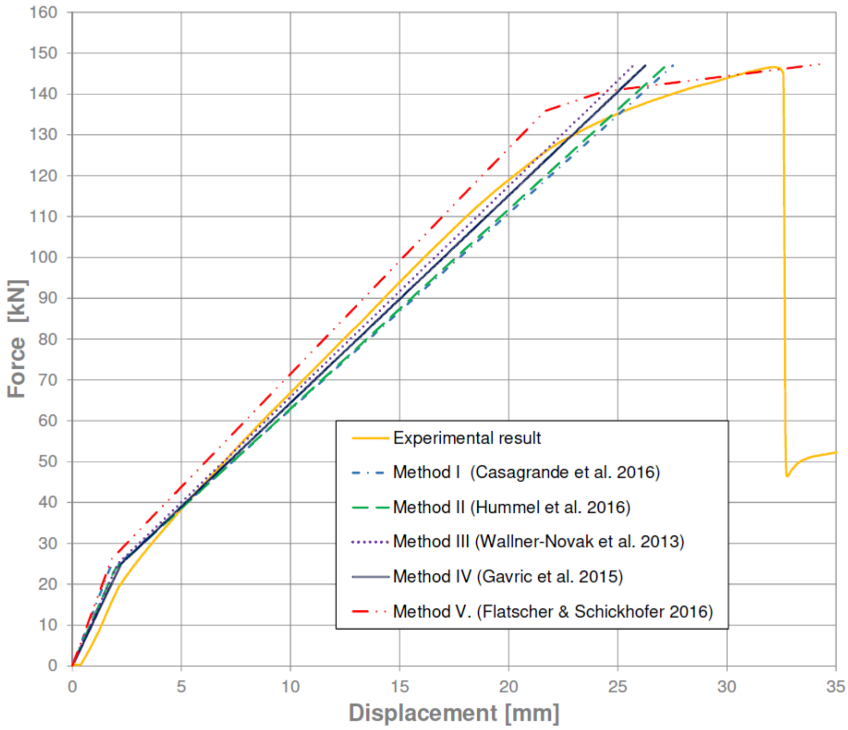

Figure 18. Comparison of test result with calculated load-deformation behavior.

From Fig. 18, it seems that for this specific shear wall configuration, all of the methods are able to predict the elastic behavior with Method V slightly overestimating, and Methods I, II and IV slightly underestimate the elastic stiffness. The method that most accurately seem to predict the elastic stiffness is Method III. It should be noted that for Methods IV and V, a linear elastic load-deformation behavior was assumed for both the hold-downs and the angle brackets, which was not proposed by the respective authors. The reason why Method V is able to predict a second linear stiffness is because the iteration of the deformation contribution of the connections utilizes the strength of each connector which cannot exceed its capacity.

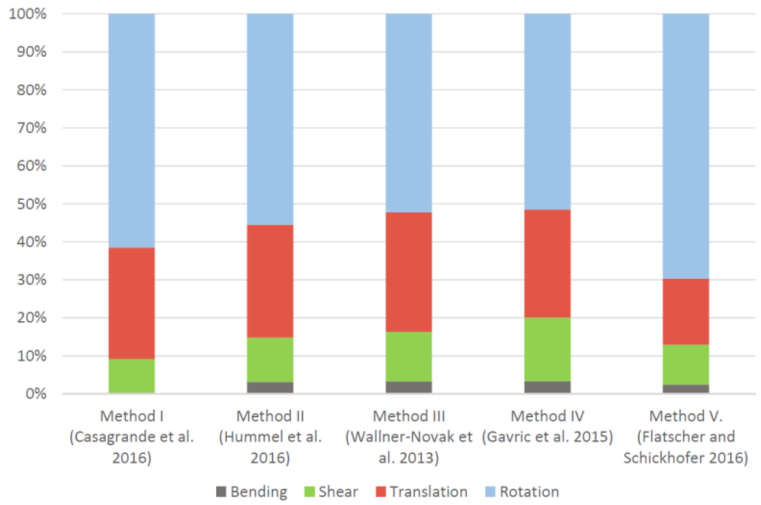

Figure 19. Illustration of displacement contribution for each method at the ultimate lateral load.

For this specific shear wall configuration, the contribution of the bending deformations to the total deformation of the shear wall is low (Fig. 19) which is due to the high flexural stiffness of the CLT material in relation to the stiffness of the connectors. Also, in this case the panel shear deformation are substantially lower than the connection based deformations.

4. DISCUSSION AND CONCLUDING REMARKS

This paper presents and discuss the methods used to assess the behavior of shear walls in term of strength and stiffness. The methods proposed in the state-of-the-art are in general quite simple, utilizing static and kinematic equilibrium based on rigid body rotation of the CLT panel to evaluate the forces in connectors. The CLT shear wall is in this paper is viewed as a single wall panel without any openings and without any connections to other vertical or horizontal panels. The methods found in the literature are exclusively based on hold-down connector and angle brackets that are mainly used to resist rotation and sliding respectively, which is the current state of practice in CLT construction. The applicability of these methods is strongly dependent on the connection system and further study is required to include other possible connection systems. The redundancy present in real structures was purposely neglected in this overview with the aim to validate simple design approaches.

4.1. Strength methods

This paper presents 10 different methods used to assess the lateral strength of CLT shear walls which is typically limited by either the lateral resistance in rotation or sliding. For the case study shear wall used in this paper, the lateral resistance based on rotation governs the behavior of the shear wall. However, it should be especially be noted that different shear wall configuration and different connection systems can have a substantial effect on the behavior of the shear wall. Therefore, the calculations presented in this paper should merely be seen as an example and a thorough study of different shear wall configurations is required in order to evaluate the analytical approach that best approximates the real shear wall behavior. The strength methods can be divided into two main groups in regards to their application:

1) *Methods A, B, C, I and J* only consider an internal lever arm between the tensile bracing and the compression zone which length mainly vary from the size of the compression zone. To resist rotation of the shear wall, only the connector furthest from the point of rotation is considered while the angle brackets are designed to exclusively resist sliding. These methods typically consider only a few variables that can be readily determined from test results or based on producer data. The simplistic use of these methods, enables quick assessment of the lateral strength of a CLT shear wall.

2) *Methods D, E, F, G, and H* does, in addition to an internal lever arm, also consider the vertical capacity of the shear connectors. Even though their application is slightly more complex, these methods are still straightforward to use and seem to more accurately model the real behavior of the CLT shear wall. The vertical strength of angle brackets must be defined, information which in some cases can be difficult to obtain as these connectors are typically used only to resist sliding.

4.2. Stiffness methods

To assess the displacement of a shear wall requires the calculation of shear and bending deformations in the CLT panel itself and the panel rocking and sliding behavior that is dependent on the stiffness of the connectors used. This paper presents five methods to assess the displacement (stiffness) of CLT shear walls. Method I is neglecting the bending deformation of the CLT panel, while the other methods consider bending even though its contribution to the total shear wall deformation is typically low. As expected, the majority of the stiffness of the CLT shear wall relies on the stiffness of the connectors themselves. The methods are quite comparable, providing similar results. However, if the connection system is changed, the results from the different contributions seem to change significantly, indicating that the models are sensitive to the vertical and horizontal stiffness of the shear connectors.

Similar to what was observed for strength assessment, the methods proposed are exemplified using one single shear wall configurations that does not fully describe the redundancy of a real structure. It is worth saying that in many practical applications it is more relevant to assess the relative stiffness of components rather than obtaining accurate results. Therefore, the usefulness of an analytical method should be related to its ability to correctly describe the stiffness as influenced by, for example, the vertical load and the connector stiffness.

5. ACKNOWLEDGEMENTS

The contents presented in this paper is part of the EU-funded COST Action FP1402 working group and part of the Norwegian project "Increased use of wood in urban areas - WOOD/BE/BETTER", funded by The Norwegian Research Council through the BIONÆR/BIONAER research program. The authors would also like to acknowledge the dedicated work of MSc student Claudio Pradel in preparing contents for parts of this paper.

6. REFERENCES

[1] EN 1995-1-1:2004/A2 Eurocode 5: Design of timber structures. Part 1-1: General. Common rules and rules for buildings. CEN, Brussels, Belgium, 2014.

[2] EN 1998-1:2004/A1 Eurocode 8: Design of structures for earthquake resistance. Part 1: General rules, seismic actions and rules for buildings. CEN, Brussels, Belgium, 2013.

[3] Moroder D. Floor diaphragms in multi-storey timber buildings. PhD Thesis, University of Canterbury, Christchurch, New Zealand, 2016.

[4] Foster RM, Reynolds TP, Ramage MH. Proposal for defining a tall timber building. Journal Structural Engineering, 2016, DOI 10.1061/(ASCE)ST.1943-541X.0001615. https://doi.org/10.1061/(ASCE)ST.1943-541X.0001615

[5] Lukacs I, Björnfot A. Structural performance of multi-story Cross-Laminated Timber (CLT) buildings. Structures and Architecture, Beyond their Limits. Guimarães, Portugal: Taylor & Francis, 2016, ISBN 978-1-138-02651-3. p. 1490-1498.

[6] Ceccotti A, Follesa M, Lauriola MP, Sandhaas C, Minowa C, Kawai N and Yasumura M. Which seismic behaviour factor for multi-storey buildings made of Cross-Laminated wooden panels? 39th CIB W18 Meeting - CIB-W18/39-15-4, 2006, Florence, Italy.

[7] Fragiacomo M, Dujic B, Sustersic I. Elastic and ductile design of multi-storey crosslam massive wooden buildings under seismic actions. Engineering Structures, 2011, 33(11): 3043-3053, doi: 10.1016/j.engstruct.2011.05.020.

[8] Follesa M, Christovasilis IP, Vassallo D, Fragiacomo M, Ceccotti A Seismic design of multi-storey CLT buildings according to Eurocode 8. Ingegneria Sismica: International Journal Earthquake Engineering, 2013, 30(4): 27-5.

[9] Ashtari S, Haukaas T, Lam F. In-plane stiffness of Cross-Laminated Timber floors. World Conference on Timber Engineering (WCTE), 2014, Quebec, Canada.

[10] ASCE 7-10: ASCE 2010. Minimum design loads for buildings and other structures. American Society of Civil Engineers, 2010; Reston, VA, ISBN 978-0-784-41291-6.

[11] International Building Code: IBC 2012. International Code Council., USA. ISBN 978-1-60983-040-3.

[12] ASCE 7-10: ASCE 2010. Minimum design loads for buildings and other structures. American Society of Civil Engineers, 2010; Reston, VA, ISBN 978-0-784-41291-6.

[13] APEGBC. Structural, fire protection and building envelope professional engineering services for 5 and 6 storey wood frame residential building projects (Mid-Rise Buildings). Association of Professional Engineers and Geoscientists of British Columbia, APEGBC Technical & Practice Bulletin, 2009, revised April 2015.

[14] Chen ZY, Chui YH, Ni C, Doudak G, Mohammad M. Load distribution in timber structures consisting of multiple lateral load resisting elements with different stiffnesses. Journal Performance of Constructed Facilities, 2014a, DOI 10.1061/(ASCE)CF.1943-5509.0000587. https://doi.org/10.1061/(ASCE)CF.1943-5509.0000587

[15] Wallner-Novak M, Koppelhuber J, Pock K. Information Brettsperrholz Bemessung Grundlagen für Statik und Konstruktion nach Eurocode. proHolz Austria, 2013, ISBN 978-3-902926-03-6.

[16] Hummel J. Displacement-based seismic design for multi-storey Cross Laminated Timber buildings. Vol. 8. Kassel University Press, 2016.

[17] Vogt T, Hummel J, Schick M, Seim W. Experimentelle Untersuchungen für innovative erdbebensichere Konstruktionen im Holzbau. Bautechnik 91, 2014, Hef 1, DOI: 10.1002/bate.201300083.

[18] Reynolds T, Foster R, Bregulla J, Chang W-S, Harris R, Ramage M. Lateral-load resistance of Cross-Laminated Timber shear walls. Journal Structural Engineering, 2017, DOI: 10.1061/(ASCE)ST.1943-541X.0001912. https://doi.org/10.1061/(ASCE)ST.1943-541X.0001912

[19] Casagrande D, Rossi S, Sartori T, Tomasi R. Proposal of an analytical procedure and a simplified numerical model for elastic response of single-storey timber shear-walls. Journal Construction and Building Materials, 2016, Volume 102, 1101–1112. https://doi.org/10.1016/j.conbuildmat.2014.12.114

[20] Tomasi R. CLT course at FPS COST Action FP1004 – Enhance mechanical properties of timber, engineered wood products and timber structures. CLT Training School, University of Trento, 15-17 April 2014.

[21] Ringhofer A. Erdbebennormung in Europa und deren Anwendung auf Wohnbauten in Holz- Massivbauweise. Master thesis, 2010, Technische Universität Graz, Austria.

[22] Schickhofer G., Ringhofer A. The seimic behaviour of buildings erected in solid timber construction | Seismic design according to EN 1998 for a 5-storey reference building in CLT. Vol. 1, TU Graz, Graz, Austria, 2011.

[23] Pei S, Lindt JVD, Popovski M. Approximate R-factor for Cross-Laminated Timber walls in multi-story buildings. Journal Architectural Engineering, 2012, Volume 19/4, 245–255. https://doi.org/10.1061/(ASCE)AE.1943-5568.0000117

[24] Pei S, Popovski M, Van de Lindt JW. Analytical study on seismic force modification factors for Cross-Laminated Timber buildings. Canadian Journal of Civil Engineering, 2013, Volume 40(9), 887–896. https://doi.org/10.1139/cjce-2013-0021

[25] Shen Y-L, Schneider J, Tesfamariam S, Stiemer SF, Mu Z-G. Hysteresis behavior of bracket connection in Cross-Laminated-Timber shear walls. Journal Construction and Building Materials, 2013, Volume 48, 980–99. https://doi.org/10.1016/j.conbuildmat.2013.07.050

[26] Karakabeyli E, Douglas B. CLT Handbook. FPInnovations, 2013, US edition, Quebec.

[27] Gavric I and Popovski M. Design models for CLT shearwalls and assemblies based on connection properties. International Network on Timber Engineering Research, 2014, INTER/47-15-4, pages 267-280.

[28] Rinaldin G and Fragiacomo M. Non-linear simulation of shaking-table tests on 3- and 7-storey X-Lam timber buildings. Journal of Engineering Structures, 2016, Volume 113, 133-148. https://doi.org/10.1016/j.engstruct.2016.01.055

[29] Schickhofer G, Bogensperger T, Moosbrugger T, Augustin M, Blaß H J, Ebner H, Ferk H, Fontana M, Frangi A, Hamm P, Jöbstl RA, Richter A, Thiel A, Traetta G and Uibel, T. BSPhandbuch Holz-Massivbauweise in Brettsperrholz Nachweise auf Basis des neuen europäischen Normenkonzepts. 2. Auflage, Verlag der Technischen Universität Graz, 2010, Graz.

[30] Flatscher G. Evaluation and approximation of timber connection properties for displacement-based analysis of CLT wall systems. Vol. 6 Monographic Series TU Graz/Timber Engineering & Technology, 2017, Graz.

[31] Tamagnone G, Rinaldin G, Fragiacomo M. A novel method for non-linear design of CLT wall systems. Journal Engineering Structures, 2017, ISSN 0141-0296. https://doi.org/10.1016/j.engstruct.2017.09.010

[32] Tomasi R. Seismic behavior of connections for buildings in CLT. Focus solid timber solutions. Proceedings of the European Conference on Cross-Laminated Timber, TU Graz, 21-22 May 2013. COST Action FP1004, pp. 138-151.

[33] Tomasi R and Smith I. Experimental characterization of monotonic and cyclic loading response of CLT panel-to-foundation angle bracket connections. Journal Materials in Civil Engineering, 2015, 27(6): 04014189(1-10), DOI: 10.1061/(ASCE)MT.1943-5533.0001144. https://doi.org/10.1061/(ASCE)MT.1943-5533.0001144

[34] Andreolli, M., Tomasi, R. Bemessung von Gebäuden in Brettsperrholzbauweise unter Erdbebenbeanspruchung. Bautechnik 93, 2016, Heft 12 (885-898).

[35] Hummel J, Seim W, Otto S. Steifigkeit und Eigenfrequenzen im Mehrgeschossingen Holzabau. Bautechnik 93, 2016**,** Hef 11, 781-794, DOI: 10.1002/bate.201500105.

[36] Gavric I, Fragiacomo M, Ceccotti A. Cyclic behaviour of CLT wall systems: Experimental tests and analytical prediction models. Journal of Structural Engineering, 2015, 141(11).

[37] Flatscher G and Schickhofer G. Displacement-based determination of laterally loaded Cross Laminated Timber (CLT) wall systems. Proceedings of the 3rd INTER Meeting - INTER/49-12-1, Graz, August 2016.

[38] Vessby J. Analysis of shear walls for multi-storey timber buildings. Doctoral Thesis No 45/2011, Linnaeus University, Växjö, Sweden.

[39] Reynolds T, Harris R, Chang W-S, Bregulla J, Bawcombe J. Ambient vibration test of Cross-Laminated Timber building. Proceedings of the Institution of Civil Engineers: Construction Materials, 2015, 168 (3), 121-131. https://doi.org/10.1680/coma.14.00047

[40] Seim W, Hummel J, Vogt T. Earthquake design of timber structures – remarks on force-based design procedures for different wall systems. Journal Engineering Structures, 2014, Volume 76, pages 124-137. https://doi.org/10.1016/j.engstruct.2014.06.037

[41] Hummel J, Seim W. Assessment of dynamic characteristics of multi-storey timber buildings. World Conference on Timber Engineering (WCTE), 2016, Vienna, Austria.

[42] Brandner R, Flatscher G, Ringhofer A, Schickhofer G, Thiel A. Cross laminated timber (CLT): overview and development. European Journal of Wood and Wood Products, 2016, 74(3): 331-351, doi: 10.1007/s00107-015-0999-5.

[43] Gavric I, Ceccotti A, and Fragiacomo M. Experimental cyclic tests on Cross-Laminated Timber panels and typical connections. Proceeding of 14th ANIDIS Conference, 2011, Politecnico di Bari, Italy.